Signature of phonon drag thermopower in periodically modulated structures

Alain Nogaret
Department of Physics, University of Bath, Bath BA2 7AY, United Kingdom

(Received 30 January 2002; revised manuscript received 2 May 2002; published 3 September 2002)

A theory is presented to interpret the phonon drag magneto-thermopower oscillations observed in a periodically modulated two-dimensional electron gas. The thermoelectric and phonon drag tensors are obtained by solving a Boltzmann equation driven by an anisotropic electron-phonon scattering rate reflecting the twofold symmetry of the Fermi surface. It is shown that commensurability oscillations in the phonon drag and the Nernst-Ettingshausen coefficients arise exclusively because of finite angle scattering events. The calculated oscillations are found to be in phase with the magnetoresistance and their magnitude is proportional to the electron-phonon anisotropy.

DOI: 10.1103/PhysRevB.66.125302 PACS number(s): 73.23.Ad, 72.20.Pa

I. INTRODUCTION

Periodically modulated two-dimensional electron gases (2DEG's) have been intensively studied over the past decade following the discovery, by Weiss *et al.*[1] of commensurability magnetoresistance oscillations. The physical origin of these oscillations is now well established from concurring theoretical pictures.[2–5] Collisions between quasiballistic electrons and the superlattice potential contribute to large corrections in the conductivity. In the presence of a magnetic field B applied perpendicular to the 2DEG, the resistance oscillates due to the cyclotron diameter at the Fermi level, $2R_c$, scaling with an integer number superlattice periods a within a phase factor. This picture was extended to the electronic heat conductivity and the *diffusion* thermopower.[6] The latter was subsequently measured using a local heating technique that allows one to study diffusion of hot electrons without heating the lattice. Commensurability thermopower oscillations were observed which were 90° out of phase compared to the resistivity oscillations, in line with the theoretical expectations.[7]

This paper investigates the voltage induced by a macroscopic heat current flowing across a lateral superlattice fabricated from a GaAs/(Al,Ga)As heterostructure. The difference from Ref. 7 is that the dominant contribution to the thermopower now arises from the *phonon drag* acting on the 2DEG rather than from the diffusion of hot electrons.[8,9] A series of magneto-drag thermopower oscillations were reported[10] that cannot be explained within the current theoretical framework that only extends to unmodulated systems.[11–13] We shall show that the potential modulation lowers the symmetry of the Fermi surface and we shall calculate its influence on the phonon drag acting on the 2DEG.[9,11,14]

The thermopower $\mathbf{S}$ is defined as $\mathbf{E}=\mathbf{S}\cdot\nabla\mathbf{T}$, where $\mathbf{E}$ is the gradient of the electrochemical potential and $\nabla\mathbf{T}$ is the temperature gradient applied to the 2DEG. Thermopower measurements are realised with no net charge current flowing through the sample so that the thermoelectric current is exactly compensated by a electric current: $\mathbf{j}=\boldsymbol{\sigma}\cdot\mathbf{E}\text{-}\mathbf{L}\cdot\nabla\mathbf{T}=\mathbf{0}$. The thermopower is then $\mathbf{S}=\boldsymbol{\sigma}^{-1}\mathbf{L}$, where $\boldsymbol{\sigma}$ and $\mathbf{L}$ are the conductivity and the thermoelectric tensor respectively. In contrast to the diffusion thermopower, the phonon drag thermopower (S^g) is an indirect means of probing the 2DEG. A temperature gradient generates a nonequilibrium phonon distribution that in turn transfers some of its momentum to the electrons.[13] Electron-phonon interactions being slow, $\tau_{\mathrm{ep}}\sim 10^{-9}$ s,[15] compared to impurity scattering, $\tau\sim 10-30$ ps, momentum is rapidly scattered away. In average, the Fermi sea is displaced in momentum space by an amount $\propto(\tau/\tau_{\mathrm{ep}})\nabla\mathbf{T}$. Miele *et al.*[11] have explicitly shown that the action of phonon drag is equivalent to that of an effective electric field directed along the temperature gradient and depending only on temperature and phonon parameters. This result implies that S^g is independent of B, it explains the absence of weak localisation effects[11] in the thermopower, S_{yy}, and the vanishingly small Nernst-Ettingshausen coefficient S_{xy}.[16] Whether the 2DEG is modulated or not is actually irrelevant because S^g remains independent of B, therefore the phonon drag is not expected to show commensurability effects. This picture has two limitations: first, electron and phonon anisotropies combine to increase the Nernst-Ettingshausen coefficient,[17] and second, the displaced electron and phonon distributions in momentum space cannot be in equilibrium because the magnetic field only acts on electrons.[18]

In the following, I shall derive a solution to Boltzmann equation driven by an anisotropic electron-phonon scattering rate. This anisotropy has a twofold symmetry that reflects the symmetry of the Fermi surface imposed by the one-dimensional grating. The thermoelectric and thermopower tensors are calculated with phonon anisotropy being introduced as a single phenomenological parameter. With this new assumption, the standard phonon drag theory[10] is capable of reproducing the commensurability oscillations seen in $\mathbf{S^g}$.

The paper is organized into three sections. The first one derives the thermoelectric tensor modified for the effects of the periodic potential. The thermopower is then calculated in the simple case of isotropic electron-phonon interaction. The second section presents an exact solution of Boltzmann equation driven by anisotropic electron-phonon scattering. Each angular harmonic contributes a corrective term to the thermopower, the leading term of which is given by the roots of a characteristic polynomial. The magnetic-field depen-

 ©2002 The American Physical Society

dence of the thermopower is calculated and results are discussed in the third section.

II. ISOTROPIC ELECTRON PHONON SCATTERING

The temperature gradient is applied along the potential modulation taken as $V(y)=V_0\cos(qy)$ where $q=2\pi/a$. This was experimentally realised by gating a 2DEG with 200-nm-wide metal finger gates with a periodicity $a=500$ nm. The electron density in the 2DEG was $2.4\times10^{15}\ \mathrm{m}^{-2}$ and the mobility $930\,000\ \mathrm{cm}^2\ \mathrm{V}^{-1}\ \mathrm{s}^{-1}$. The modulation had a piezoelectric origin,[19] and its amplitude, calculated from the width of the positive magnetoresistance, was found to be $V_0=1$ mV. The phonon drag thermopower S_{yy} and the Nernst-Ettingshausen coefficient S_{yx} are obtained by measuring the voltage drop parallel and perpendicular to the temperature gradient. The electron-phonon scattering rate responsible for phonon drag is given by[11]

$$\left.\frac{\partial f_k}{\partial t}\right|_{\mathrm{ph}}=\frac{\partial f_{\mathbf{k}}^0}{\partial\varepsilon_{\mathbf{k}}}\sum_\lambda \frac{m^* s_\lambda\Lambda_\lambda}{\tau_{ep}^\lambda}\mathbf{v_k}\frac{\boldsymbol{\nabla}\mathbf{T}}{T}, \tag{1}$$

where $\partial f_{\mathbf{k}}^0/\partial\varepsilon_{\mathbf{k}}$ is the derivative of the Fermi-Dirac function, $m^*=0.067m_0$ is the electron effective mass, s_λ is the phonon velocity of the acoustic mode λ, Λ_λ is the phonon mean free path, and $\mathbf{v_k}$ is the velocity of an electron in state $\mathbf{k}$. At 4 K, the 2DEG is highly degenerate hence $\partial f_{\mathbf{k}}^0/\partial\varepsilon_{\mathbf{k}}$ may be replaced by $-\delta(\varepsilon_{\mathbf{k}}-\varepsilon_F)$ in Eq. (1). An electron on the Fermi surface travelling with velocity $v(y)$ along the direction $\mathbf{u_1}=(\cos\phi,\sin\phi)$ will be subject to a phonon drag W^0,

$$W^0(\phi,y)=\int_0^\infty dkk\frac{-2e}{4\pi^2}\left.\frac{\partial f}{\partial t}\right|_{\mathrm{ph}}=-\frac{\nu(y)}{2\pi}\frac{\sigma_0S_0}{D_0}\mathbf{u_1}\cdot\boldsymbol{\nabla}\mathbf{T}, \tag{2}$$

where $\sigma_0=n_se^2\tau/m^*$ is the Drude conductivity, $D_0=1/2\nu_F^2\tau$ and

$$S_0=-\sum_\lambda\frac{m^*s_\lambda\Lambda_\lambda}{e\tau_{ep}^\lambda T}$$

is the isotropic phonon drag thermopower, ν_F is the Fermi velocity of the unmodulated 2DEG and e is the electron charge. The thermoelectric current is $\mathbf{j}=\int_0^a(dy/a)\int_0^{2\pi}d\phi\ f^0(y,\phi)\nu\mathbf{u_1}$ where f^0 is the charge distribution function solution of Boltzmann equation:

$$\mathcal{L}f^0=\left\{\nu(y)\mathbf{u_1}\cdot\boldsymbol{\nabla}_{\mathbf{r}}+[\nu'(y)\cos\phi+\omega_c]\frac{\partial}{\partial\phi}+\frac{1}{\tau}\left[1-\int_0^{2\pi}\frac{d\phi}{2\pi}\right]\right\}f^0(y,\phi)=W^0(y,\phi). \tag{3}$$

$\omega_c=eB/m^*$ is the cyclotron frequency. Equation (3) is mathematically identical to that governing the resistivity problem previously solved by Beenakker;[2] therefore, only key steps of the calculation will need to be recalled here. A function $F^0(y,\phi)$ is introduced as

$$2\pi f^0(y,\phi)=-\frac{\nu(y)\tau}{D_0}S_0\mathbf{u_1}\boldsymbol{\sigma}_\mathbf{1}^0\boldsymbol{\nabla}\mathbf{T}-F^0(y,\phi)\sigma_1S_0[\omega_c\tau(\nabla T)_x+(\nabla T)_y], \tag{4}$$

which has to satisfy

$$\mathcal{L}F^0=eE(y)/\varepsilon_F \tag{5}$$

where $E(y)=-dV(y)/dy$ is the periodic electric field. $\boldsymbol{\sigma}_\mathbf{n}^0$ is the unperturbed conductivity tensor of order n ($n=1,2...$) which has components $\sigma_{xx}=\sigma_{yy}=\sigma_n$ and $\sigma_{xy}=-\sigma_{yx}=-n\omega_c\tau\sigma_n$ where $\sigma_n=\sigma_0/[1+(n\omega_c\tau)^2]$. It will also be useful to introduce the vector $\mathbf{u}_n=[\cos(n\phi),\sin(n\phi)]$. The current integrals are simplified by observing that the only non vanishing contributions arise from the terms in $\cos\phi$ and $\sin\phi$ in the Fourier expansion of F^0. Inserting this expansion into Eq. (5) gives the Fourier coefficients of $\cos\phi$ and $\sin\phi$, and one obtains

$$\int_0^a\frac{dy}{a}\int_0^{2\pi}\frac{d\phi}{2\pi}\nu(y)F^0(y,\phi)\mathbf{u_1}=K(\omega_c\tau,-1). \tag{6}$$

The ratio $\eta=eV_0/\varepsilon_F$ is small ($\eta=0.12$) and, to first order in η, Eq. (5) has an exact solution whose oscillatory dependence is given by Bessel functions of complex order,[20,21]

$$K=\frac{D_0}{1+(\omega_c\tau)^2}\int_0^a\frac{dy}{a}\int_0^{2\pi}\frac{d\phi}{2\pi}\frac{eE(y)}{\varepsilon_F}F^0(y,\phi)=\frac{\eta^2}{4}\frac{(ql)^2}{1+(\omega_c\tau)^2}\frac{J_{i/\omega_c\tau}(qR_c)J_{-i/\omega_c\tau}(qR_c)}{\dfrac{\sinh(\pi/\omega_c\tau)}{(\pi/\omega_c\tau)}-J_{i/\omega_c\tau}(qR_c)J_{-i/\omega_c\tau}(qR_c)}, \tag{7}$$

where $R_c=m^*\nu_F/eB$. Combining Eqs. (4) and (6) one finds the thermoelectric current to be: $\mathbf{j}=-S_0\boldsymbol{\sigma}_\mathbf{1}\boldsymbol{\nabla}\mathbf{T}$, where

$$\sigma_1=\sigma_1\begin{pmatrix}1+K(\omega_c\tau)^2 & -[1-K](\omega_c\tau)\\ [1-K](\omega_c\tau) & [1-K]\end{pmatrix} \tag{8}$$

is the Drude conductivity tensor modified by the oscillatory contribution from the grating. The thermoelectric tensor is identified as $\mathbf{L_1}=S_0\boldsymbol{\sigma}_\mathbf{1}$ and, recalling the condition $\boldsymbol{\sigma}_\mathbf{1}\mathbf{E}-\mathbf{L_1}\boldsymbol{\nabla}\mathbf{T}=\mathbf{0}$, the phonon drag thermopower follows as $\mathbf{S_1}=\boldsymbol{\sigma}_\mathbf{1}^{-1}\mathbf{L_1}=S_0\mathbf{1}$.

This result demonstrates that the periodic modulation has no effect on the *phonon drag thermopower*. The lack of oscillatory dependence suggests that some ingredient may be missing in the initial assumptions. For instance, the formation of Brillouin minizones due to the periodicity of the superlattice potential is assumed to have no effect on the scattering rate. The folding of energy dispersion curves fractures the Fermi surface into a complex pattern of arcs of circle exhibiting twofold symmetry as shown in Fig. 1. Such an anisotropy will be passed onto the electron-phonon interaction since it depends strongly on the density of available states on the Fermi surface. In particular, the scattering rate increases dramatically for transitions between opposite edges of the Fermi surface where the density of states is divergent

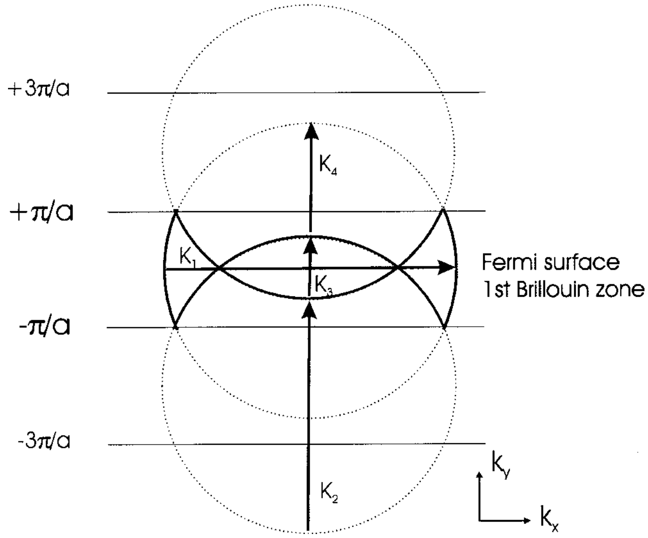

FIG. 1. Schematic view of the Fermi surface in the presence of a small 1D potential modulation. $K_1,\ldots,K_4$ label the acoustic-phonon-mediated transitions for which the scattering rate diverges (Kohn anomalies).

(Kohn anomalies). Kohn anomalies are, for example, well known for enhancing the phonon drag thermopower around 10 K.[8] Figure 1 shows that longitudinal (K_2,K_3,K_4) and transverse transitions (K_4) involve phonons with different wavevectors suggesting some degree of angular anisotropy will be present in the electron-phonon scattering. The Fermi density of states will remain largely unaffected by the magnetic field, since Landau levels are not formed. The independence of the electron-phonon anisotropy on the magnetic field may therefore be assumed.[22] These considerations suggest that the scattering rate can be expanded according to its angular harmonics as

$$S_a=S_0\left[\frac{a_0}{2}+\sum_{n=1}^{\infty} a_n\cos(n\phi)+b_n\sin(n\phi)\right]. \tag{9}$$

III. ANISOTROPIC ELECTRON-PHONON SCATTERING

The new driving term $W(y,\phi)$ is obtained by substituting S_a [Eq. (9)] into Eq. (2):

$$\begin{aligned}W(y,\phi)=&-\frac{\nu(y)}{2\pi}\frac{\sigma_0S_0}{D_0}\left\{\frac{a_0}{2}\mathbf{u_1}\cdot\nabla\mathbf{T}+\frac{1}{2}\{\cos\phi(a_2(\nabla T)_x\right.\\&+b_2(\nabla T)_y)+\sin\phi[b_2(\nabla T)_x-a_2(\nabla T)_y]\}\\&+\frac{1}{2}\sum_{n=2}^{\infty}\cos(n\phi)[(a_{n+1}+a_{n-1})(\nabla T)_x\\&+(b_{n+1}-b_{n-1})(\nabla T)_y]+\sin(n\phi)[(b_{n+1}+b_{n-1})\\&\left.\times(\nabla T)_x-(a_{n+1}-a_{n-1})(\nabla T)_y]\right\}.\end{aligned} \tag{10}$$

One may seek the solution of $\mathcal{L}f(y,\phi)=W(y,\phi)$ as the sum of the partial electronic responses to each angular harmonic in $W(y,\phi)$. Using the linearity of the Liouville operator, $f(y,\phi)=f_1^0+f_1+\Sigma_{n=2}^{\infty}f_n$. It follows that each harmonic contributes independently to the thermoelectric current, the thermoelectric and the thermopower tensors.

The partial responses to the driving terms in $\cos\phi$ and $\sin\phi$ were solved in Sec. I. The distribution function f_1^0, corresponding the first term in Eq. (10), is obtained by replacing $\nabla\mathbf{T}\rightarrow(a_0/2)\nabla\mathbf{T}$ in Eq. (4). In the same way, f_1 is obtained by substituting $\nabla\mathbf{T}\rightarrow(a_2(\nabla T)_x+b_2(\nabla T)_y,b_2(\nabla T)_x-a_2(\nabla T)_y)$ in Eq. (4). The thermopower contribution from the first two terms in Eq. (10) is found to be

$$\mathbf{S}_1=\frac{S_0}{2}\begin{pmatrix}a_0+a_2 & b_2\\ b_2 & a_0-a_2\end{pmatrix}. \tag{11}$$

The electronic response to harmonics $n\geqslant 2$ is governed by

$$\begin{aligned}\mathcal{L}f_n(y,\phi)=&-\frac{\nu(y)}{2\pi}\frac{\sigma_0S_0}{D_0}\frac{1}{2}\{\cos(n\phi)\\&\times[(a_{n+1}+a_{n-1})(\nabla T)_x+(b_{n+1}-b_{n-1})(\nabla T)_y]\\&+\sin(n\phi)[(b_{n+1}+b_{n-1})(\nabla T)_x\\&-(a_{n+1}-a_{n-1})(\nabla T)_y]\}.\end{aligned} \tag{12}$$

A function F_n is defined as

$$2\pi f_n(y,\phi)=-\frac{\nu(y)\tau}{D_0}S_0\mathbf{u}_n\boldsymbol{\sigma}_n^0\nabla\mathbf{T}'-\sigma_nS_0F_n(y,\phi),$$

where

$$\nabla\mathbf{T}'=\frac{1}{2}\begin{pmatrix}a_{n+1}+a_{n-1} & b_{n+1}-b_{n-1}\\ b_{n+1}+b_{n-1} & -a_{n+1}+a_{n-1}\end{pmatrix} \tag{13}$$

with the condition that

$$\begin{aligned}\mathcal{L}F_n=&\frac{eE(y)}{\varepsilon_F}\frac{1}{2\sigma_n}\left\{\frac{n+1}{n-1}\frac{\partial\mathbf{u}_{n-1}}{\partial\phi}\right.\\&\left.+\frac{n-1}{n+1}\frac{\partial\mathbf{u}_{n+1}}{\partial\phi}\right\}\boldsymbol{\sigma}_n^0\nabla\mathbf{T}'\quad(n\geqslant 2).\end{aligned} \tag{14}$$

Substitution (13) removes all spatial harmonics other than the fundamental frequency in the function F_n. One may therefore seek solutions of Eq. (14) in the form: $F_n(y,\phi)=(\eta/v_F)\Sigma_{m=-\infty}^{+\infty}\Psi_me^{i(qy+m\phi)}+\text{cc.}$[21] Inserting this expansion into Eq. (14) gives a recursion formula generating the entire set of Ψ_m,

$$\alpha_m\Psi_m=\Psi_{m+1}-\Psi_{m-1}+\beta_m, \tag{15}$$

where

$$\alpha_m=\frac{2}{ql}(im\omega_c\tau+1-\delta_{m,0}),$$

$$\beta_m=\frac{n+1}{4}[\delta_{m,n-1}(V_x-iV_y)-\delta_{m,-(n-1)}(V_x+iV_y)]$$
$$+\frac{n-1}{4}[\delta_{m,n+1}(V_x-iV_y)-\delta_{m,-(n+1)}(V_x+iV_y)],$$

$$n=2,3..., \quad m=\ldots-2,-1,0,+1,+2.... \tag{16}$$

A vector is introduced which is defined as $\mathbf{V}\equiv\boldsymbol{\sigma}_n^0\boldsymbol{\nabla}\mathbf{T}'/\sigma_n$. Mirlin and Wölfle observed[20,21] that equations of the type of Eq. (15), albeit with no driving term ($\beta_m=0$), are satisfied by Bessel functions of complex order. The solutions of Eq. (15) (with $\beta_m=0$) are: $\Psi_m=(i)^mJ_{m-i(1-\delta_{m,0})/\omega_c\tau}(qR_c)$. These may be computed in the form of continued fractions.[23]

$$i\frac{J_{1-}}{J_-}=\cfrac{-1}{\alpha_1+\cfrac{1}{\alpha_2+\cfrac{1}{\alpha_3\ldots}}}, \quad -i\frac{J_{1+}}{J_+}=\cfrac{-1}{\alpha_{-1}+\cfrac{1}{\alpha_{-2}+\cfrac{1}{\alpha_{-3}\cdots}}} \tag{17}$$

where the shorthand notation $J_{1\pm}\equiv J_{1\pm i/(\omega_c\tau)}(qR_c)$ and $J_\pm\equiv J_{\pm i/(\omega_c\tau)}(qR_c)$ is being used.[21] If electron-phonon interaction has a twofold symmetry, the Fourier coefficients in a_2 and b_2 dominate in the Fourier expansion (9). In the first instance, one may neglect the contribution of higher angular harmonics [Eqs. (4), (8), etc.] and solve Eq. (15) driven by the second harmonic only. This approach limits the number of fitting parameters to two (one if $b_2=0$) In these conditions, $\mathbf{V}$ will have non zero components if $n=3$ ($n=1$ is already accounted for). Equation (16) shows that β_m will be finite for $m=\pm2$ and ±4. The solutions of Eq. (15) therefore take the form

$$\frac{\Psi_1}{\Psi_0}=\cfrac{-1}{\alpha_1+\cfrac{1-\beta_2/\Psi_1}{\alpha_2+\cfrac{1}{\alpha_3+\cfrac{1-\beta_4/\Psi_3}{\alpha_4+\cdots}}}}, \quad \frac{\Psi_{-1}}{\Psi_0}=\cfrac{+1}{\alpha_{-1}+\cfrac{1+\beta_{-2}/\Psi_{-1}}{\alpha_{-2}+\cfrac{1}{\alpha_{-3}+\cfrac{1+\beta_{-4}/\Psi_{-3}}{\alpha_{-4}+\cdots}}}}. \tag{18}$$

Simplifications occur by observing that, for $m=0$, Eq. (15) gives $\Psi_{-1}=\Psi_1$. Second, coefficients with negative values of m are eliminated using: $\alpha_{-m}=\alpha_m^*$ and $\beta_{-m}=-\beta_m^*$. Third Ψ_3 (Ψ_{-3}) relates to Ψ_0 and Ψ_1 via $\Psi_3=(\alpha_1\alpha_2+1)\Psi_1+\alpha_2\Psi_0-\beta_2$ $[\Psi_{-3}=(\alpha_1^*\alpha_2^*+1)\Psi_1-\alpha_2^*\Psi_0-\beta_2^*]$. These manipulations reduce Eqs. (18) to a system of two equations with two complex unknowns Ψ_0 and Ψ_1.

Once Ψ_1 is known, the thermoelectric current immediately follows from

$$\mathbf{j}=-\sigma_nS_0\int_0^a\frac{dy}{a}\int_0^{2\pi}\frac{d\phi}{2\pi}F_n(y,\phi)\,v(y)\,\mathbf{u_1}. \tag{19}$$

The Fermi velocity $v(y)=v_F\sqrt{1+\eta\cos(qy)}\cong v_F+v_F(\eta/2)\cos(qy)+O(\eta^2)$ is well approximated by its two leading terms since $\eta\ll1$. Equation (19) is then easily integrated, and I find

$$j_x=-\sigma_nS_0\frac{\eta^2}{4}\mathrm{Re}[\Psi_1],$$
$$j_y=+\sigma_nS_0\frac{\eta^2}{4}\mathrm{Im}[\Psi_1]. \tag{20}$$

It should be remarked that Eq. (6) cannot be used here due to the coupling to higher ($n>1$) harmonics. This is the reason why the current must be calculated from Ψ_1 rather than from Ψ_0.[2,21] Considering Eqs. (17) and (18), one notes that the sequence of ratios continuing beyond α_4 (α_{-4}) is common to both equations. The sequence of equations (17) is then substituted into Eq. (18) which, after some algebra, reduces to a nonlinear system in ψ_0 and ψ_1:

$$\alpha_r\Psi_1^2+\beta_r\Psi_0^2+i\gamma_i\Psi_0\Psi_1-\delta_r\Psi_1-i\rho_i\Psi_0+\kappa_r=0,$$
$$\alpha_i\Psi_1^2+\beta_i\Psi_0^2-i\gamma_r\Psi_0\Psi_1-\delta_i\Psi_1+i\rho_r\Psi_0+\kappa_i=0, \tag{21}$$

where α_r, α_i, β_r, $\beta_i\ldots Z_r$, Z_i are the real and imaginary parts of

$$\alpha=\alpha_1\alpha_2+1,$$
$$\beta=-i\alpha_2(J_{1-}/J_-),$$
$$\gamma=\alpha_2+\alpha\beta/\alpha_2,$$
$$\delta=\beta_2[1+\alpha Z], \tag{22}$$
$$\rho=\beta_2[\beta/\alpha_2+\alpha_2Z],$$
$$\kappa=\beta_2^2Z,$$

$$Z=\frac{1}{2}\{(3+\alpha_2\alpha_3)-\beta(3\alpha_1+\alpha_3\alpha)/\alpha_2\}.$$

β_4 has been replaced using the fact that, for $n=3$, Eq. (16) gives $\beta_4=0.5\beta_2$. The real and imaginary parts α_r, α_i, β_r,

$\beta_i \ldots \kappa_r$, κ_i are obtained by summing and subtracting each coefficient and its complex conjugate. This operation when applied to J_{1-}/J_- produces two terms $R_+ = (J_{1+}J_- + J_{1-}J_+)/J_+J_-$ and $R_- = i(J_{1+}J_- - J_{1-}J_+)/J_+J_-$ which are conveniently evaluated from the series expansion of the Bessel product:[24]

$$J_\nu(z)J_\mu(z) = \left(\frac{1}{2}z\right)^{\nu+\mu} \sum_{k=0}^{\infty} \frac{(-1)^k \Gamma(\nu+\mu+2k+1)\left(\frac{1}{4}z^2\right)^k}{\Gamma(\nu+k+1)\Gamma(\mu+k+1)\Gamma(\nu+\mu+k+1)k!}. \tag{23}$$

I find

$$J_{1+}J_- \pm J_{1-}J_+ = -\frac{1}{qR_c}\sum_{k=1}^{\infty} \frac{(-1)^k \Gamma(2k+1)\left(\frac{1}{2}qR_c\right)^{2k}}{\Gamma(i/\omega_c\tau+k+1)\Gamma(-i/\omega_c\tau+k+1)\Gamma(k+1)k!}[(k-i/\omega_c\tau)\pm(k+i/\omega_c\tau)], \tag{24}$$

from which R_+ and R_- are identified as

$$\begin{aligned} R_+ &= -\frac{d}{d(qR_c)}\ln(J_+J_-) \\ &\sim \frac{1}{qR_c} - \frac{\cos(2qR_c)\mathrm{sgn}(B)}{\cos^2(|qR_c|-\pi/4)+\sinh^2[\pi/(2\omega_c\tau)]}, \\ &\qquad |qR_c| \gg 1 \end{aligned} \tag{25}$$

and

$$\begin{aligned} R_- &= \frac{2}{ql}\left\{\frac{\sinh(\pi/\omega_c\tau)/(\pi/\omega_c\tau)}{J_+J_-} - 1\right\} \\ &\sim \frac{\sinh(\pi/\omega_c\tau)\mathrm{sgn}(B)}{\cos^2(|qR_c|-\pi/4)+\sinh^2[\pi/(2\omega_c\tau)]} - \frac{2}{ql}, \\ &\qquad |qR_c| \gg 1. \end{aligned} \tag{26}$$

The Bessel functions are well approximated by their asymptotic expansion since $|qR_c| \gg 1$ holds in the range of magnetic fields where the commensurability oscillations are observed. Using Eq. (23), it is easy to verify that the product $J_+J_- \sim (2/\pi|qR_c|)\{\cos^2(|qR_c|-\pi/4)+\sinh^2[\pi/(2\omega_c\tau)]\}$ must be an even function of B, which is the reason for taking the modulus of qR_c. α_r, α_i, β_r, $\beta_i \ldots Z_r$, Z_i are listed in Appendix A. Either equation in Eqs. (21) may be viewed as a second degree polynomial in Ψ_0 with roots depending on Ψ_1. These roots are calculated analytically in one equation and then eliminated by substitution into the other. The result is a characteristic polynomial in Ψ_1 whose coefficients are *all real* and are listed in Appendix B:

$$c_4\Psi_1^4 + c_3\Psi_1^3 + c_2\Psi_1^2 + c_1\Psi_1 + c_0 = 0 \tag{27}$$

Since Ψ_1 is a nonlinear function of $\mathbf{\nabla T}$, the tensor notation will, in general, be invalid for expressing quantities derived from it. However most experiments are concerned with temperature gradients applied either along x or y but not along both directions *simultaneously*. In this specific case, the thermoelectric current components j_x and j_y [Eqs. (20)] may still be presented in the tensor form:

$$\mathbf{L_3} = \sigma_3 S_0 \frac{\eta^2}{4}\begin{pmatrix} \mathrm{Re}\{\Psi_1[(\nabla T)_x=1,(\nabla T)_y=0]\} & \mathrm{Re}\{\Psi_1[(\nabla T)_x=0,(\nabla T)_y=1]\} \\ -\mathrm{Im}\{\Psi_1[(\nabla T)_x=1,(\nabla T)_y=0]\} & -\mathrm{Im}\{\Psi_1[(\nabla T)_x=0,(\nabla T)_y=1]\} \end{pmatrix}. \tag{28}$$

The corresponding thermopower contribution is

$$\mathbf{S_3} = \boldsymbol{\sigma}_1^{-1}\mathbf{L_3}, \tag{29}$$

and the total thermopower is given by the sum of contributions (11) and (29) is $\mathbf{S} = \mathbf{S_1} + \mathbf{S_3}$.

IV. RESULTS AND DISCUSSION

The roots of Eq. (27) are calculated numerically for each value of B. A polynomial root-finder implementing the Hessenberg method[25] was used for its robust convergence and its appropriateness to our type of polynomial. The model parameters consider a unit temperature gradient along the y axis: $[(\nabla T)_x = 0, (\nabla T)_y = 1]$. b_2 is set to zero, thus indicating that the principal axes of anisotropy in Fig. 1 correspond to the x and y axes. Numerical results show that Eq. (27) admits two real and two complex roots. Real roots imply that no current will flow parallel to the temperature gradient, a physically meaningless proposition. The physical answer is given by the complex root for which the thermoelectric tensor satisfies Osanger symmetry rules. The symmetry of the root is itself determined by the coefficients of the polyno-

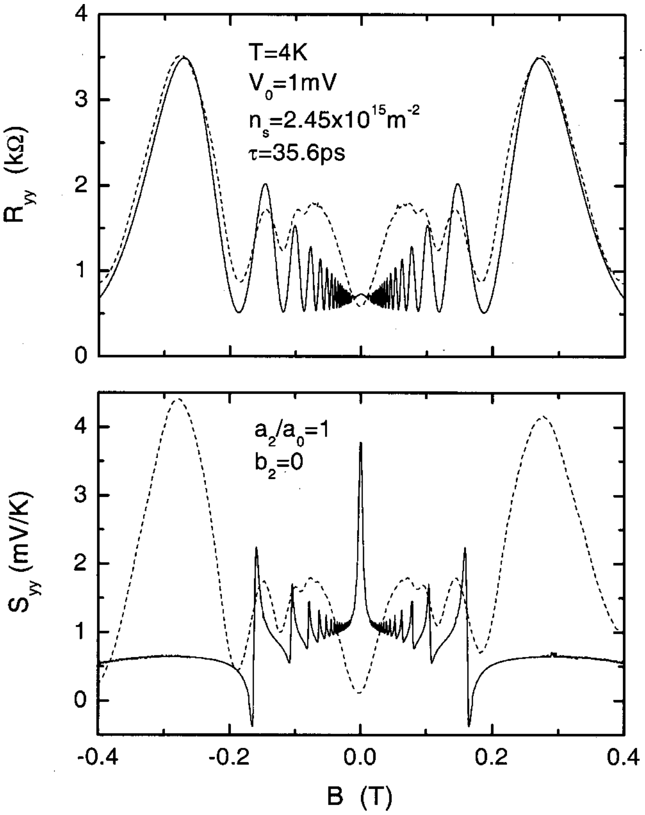

FIG. 2. Top panel: theoretical (full line) and experimental (dashed line) magnetoresistance of a lateral superlattice with period $a=500$ nm. The Drude resistance (460Ω) was calculated from the values of τ and n_s and a hall bar aspect ratio of 20; no fitting parameter was used in the theoretical curve. Bottom panel: theoretical (full line) and experimental (dashed line) phonon drag thermopower of the same lateral superlattice. The fitting parameters to the thermopower amplitude are $a_0=a_2=40\pm20$ $(b_2=0)$.

mial. It may be shown that c_4, c_2, and c_0 are even functions of B while c_3 and c_1 are odd functions of B.[26] It follows that real part the root, giving L_{xy}, is antisymmetric with respect to B, as expected. The sign of the imaginary part is chosen so that L_{xy} and L_{yy} have opposite sign when $B>0$ and the same sign when $B<0$.

The theoretical thermopower S_{yy} is plotted together with the experimental trace in the lower panel of Fig. 2 whereas the top panel compares the theoretical and experimental resistance. Comparing the experimental peak positions in the top and bottom panels shows that the phonon drag thermopower oscillates in phase with the resistance. One notes an anti-symmetric component in the experimental thermopower. Now considering the theoretical trace, commensurability thermopower oscillations arise because of the anisotropy in the scattering. The magnitude of these oscillations is proportional to a_2: if the principal scattering axis is along the x axis ($a_2>0$) S_{yy} oscillates in phase with R_{yy} and out of phase otherwise. The isotropic thermopower was evaluated as $S_0\sim220$ μV/K using a phonon mean free path equal to the etched sample length, $\Lambda=1$ mm. The vertical fit to the experimental thermopower then gave $a_2=a_0=40\pm20$ indicating that the magnitude of the oscillations is a relatively small fraction of S_0. As shown in Fig. 2, the shape of the peaks in S_{yy} is different, in particular the last oscillation is strongly attenuated in the theoretical trace. At vanishing magnetic fields, both the thermopower and the resistance show a peak not observed in the experimental data. This is because our description does not account for the channeling of open electron orbits that gives the positive magnetoresistance at low magnetic field. In order to investigate the sensitivity of phonon drag to the smoothness of the interface, we have measured the thermopower after scribing the sample surface between the heater and the Hall bar. The presence of the cut was found to dampen the amplitude of the oscillations very strongly. This outlines the importance of having a large mean free path for phonon modes travelling parallel to the sample surface.[27]

In summary, commensurability oscillations in the phonon drag thermopower of periodically modulated structures were shown to arise from the anisotropy of the electron-phonon interaction. The contribution of higher scattering harmonics $(n>2)$ was neglected because it decays as $1/n^2$. Their effect could nevertheless be calculated along similar lines but this would only be useful if the spectrum of Fourier harmonics was known. In agreement with Ref. 17, our results show that both electron ($\eta\neq0$) and phonon anisotropy ($a_2,b_2\neq0$) are required for the phonon drag thermopower to exhibit a magnetic-field dependence.

ACKNOWLEDGMENTS

I wish to acknowledge useful discussions with Dr A. Pogosov. I also thank EPSRC and the Royal Society (UK) for support.

APPENDIX A

The coefficients of Eqs. (21) are

$$\alpha_r=1+\left(\frac{2}{ql}\right)^2[1-2(\omega_c\tau)^2], \tag{nyA1}$$

$$\alpha_i=\left(\frac{2}{ql}\right)^2 3\omega_c\tau, \tag{A2}$$

$$\beta_r=\frac{1}{ql}[2(\omega_c\tau)R_+ + R_-], \tag{A3}$$

$$\beta_i=\frac{1}{ql}[2(\omega_c\tau)R_- - R_+], \tag{A4}$$

$$\gamma_r=\left(\frac{2}{ql}\right)+\frac{\alpha_i}{2}R_+ + \frac{\alpha_r}{2}R_-, \tag{A5}$$

$$\gamma_i=\left(\frac{2}{ql}\right)(2\omega_c\tau)+\frac{\alpha_i}{2}R_- - \frac{\alpha_r}{2}R_+, \tag{A6}$$

$$Z_r=\frac{1}{2}\left\{3+\left(\frac{2}{ql}\right)^2(1-6(\omega_c\tau)^2)-\left(\frac{1}{ql}\right)\{[3\omega_c\tau(1+\alpha_r)+\alpha_i]R_+ +(3-3\alpha_i\omega_c\tau+\alpha_r)R_-\}\right\}, \tag{A7}$$

$$Z_i=\frac{1}{2}\left\{\left(\frac{2}{ql}\right)^2 5\omega_c\tau-\left(\frac{1}{ql}\right)[(3\omega_c\tau(1+\alpha_r)+\alpha)R_- -(3-3\alpha_i\omega_c\tau+\alpha_r)R_+]\right\}, \tag{A8}$$

$$\delta_r=V_x[1+\alpha_r Z_r-\alpha_i Z_i]+V_y[\alpha_r Z_i+\alpha_i Z_r], \tag{A9}$$

$$\delta_i=V_x[\alpha_r Z_i+\alpha_i Z_r]-V_y[1+\alpha_r Z_r-\alpha_i Z_i], \tag{A10}$$

$$\rho_r=\frac{V_x}{2}R_- -\frac{V_y}{2}R_+ +\left(\frac{2}{ql}\right)[V_x(Z_r-2\omega_c\tau Z_i)+V_y(Z_i+2\omega_c\tau Z_r)], \tag{A11}$$

$$\rho_i=-\frac{V_x}{2}R_+ -\frac{V_y}{2}R_- +\left(\frac{2}{ql}\right)[V_x(Z_i+2\omega_c\tau Z_r)-V_y(Z_r-2\omega_c\tau Z_i)], \tag{A12}$$

$$\kappa_r=Z_r(V_x^2-V_y^2)+2Z_iV_xV_y, \tag{A13}$$

$$\kappa_i=Z_i(V_x^2-V_y^2)-2Z_rV_xV_y. \tag{A14}$$

APPENDIX B

The coefficients of the characteristic polynomial [Eq. (27)] are

$$c_4\equiv(\beta_r\alpha_i-\beta_i\alpha_r)^2-(\alpha_r\gamma_r+\alpha_i\gamma_i)(\beta_r\gamma_r+\beta_i\gamma_i), \tag{B1}$$

$$c_3\equiv(\beta_r\gamma_r+\beta_i\gamma_i)(\gamma_r\delta_r+\gamma_i\delta_i)+2\alpha_r\rho_r(\beta_r\gamma_r+\beta_i\gamma_i)+2\beta_i\rho_i(\alpha_r\gamma_r+\alpha_i\gamma_i)+(\beta_r\alpha_i-\beta_i\alpha_r)\{2(\beta_i\delta_r-\beta_r\delta_i)+(\rho_r\gamma_i+\rho_i\gamma_r)\}, \tag{B2}$$

$$c_2\equiv2(\beta_r\alpha_i-\beta_i\alpha_r)(\beta_r\kappa_i-\beta_i\kappa_r)+(\beta_i\delta_r-\beta_r\delta_i)^2-(\beta_i\rho_i+\beta_r\rho_r)(\rho_i\alpha_i+\rho_r\alpha_r)-(\beta_r\gamma_r+\beta_i\gamma_i)(\gamma_r\kappa_r+\gamma_i\kappa_i)-(\beta_r\delta_i+\beta_i\delta_r)(\rho_r\gamma_i+\rho_i\gamma_r)-2(\beta_r\rho_r\gamma_r\delta_r+\beta_i\rho_i\gamma_i\delta_i), \tag{B3}$$

$$c_1\equiv(\beta_r\rho_r+\beta_i\rho_i)(\rho_r\delta_r+\rho_i\delta_i)+2\gamma_r\kappa_r(\beta_r\rho_r+\beta_i\rho_i)+2\beta_i\gamma_i(\rho_r\kappa_r+\rho_i\kappa_i)+(\beta_r\kappa_i-\beta_i\kappa_r)\{2(\beta_i\delta_r-\beta_r\delta_i)+(\rho_r\gamma_i+\rho_i\gamma_r)\}, \tag{B4}$$

$$c_0\equiv(\beta_r\kappa_i-\beta_i\kappa_r)^2-(\kappa_r\rho_r+\kappa_i\rho_i)(\beta_r\rho_r+\beta_i\rho_i). \tag{B5}$$

[1] D. Weiss, K. von Klitzing, K. Ploog, and G. Weimann, Europhys. Lett. **8**, 179 (1989).
[2] C. W. J. Beenakker, Phys. Rev. Lett. **62**, 2020 (1989).
[3] R. R. Gerhardts, D. Weiss, and K. von Klitzing, Phys. Rev. Lett. **62**, 1173 (1989).
[4] R. W. Winkler, J. P. Kotthaus, and K. Ploog, Phys. Rev. Lett. **62**, 1177 (1989).
[5] P. Streda and A. H. McDonald, Phys. Rev. B **41**, 11 892 (1990).
[6] F. M. Peeters and P. Vasilopoulos, Phys. Rev. B **42**, 5899 (1990); F. M. Peeters and P. Vasilopoulos, Phys. Rev. B **46**, 4667 (1992).
[7] R. Taboryski, B. Brosh, M. Y. Simmons, D. A. Ritchie, C. J. B. Ford, and M. Pepper, Phys. Rev. B **51**, 17 243 (1995).
[8] B. L. Gallagher and P. N. Butcher, *Handbook on Semiconductors*, edited by P. T. Langsberg (Amsterdam, Elsevier, 1992), Vol. 1.
[9] R. Fletcher, Semicond. Sci. Technol. **14**, R1 (1999).
[10] D. Uzur, A. Nogaret, A. Pogosov, S. J. Bending, H. A. Beere, and D. A. Ritchie (unpublished).
[11] A. Miele, R. Fletcher, E. Zaremba, Y. Feng, C. T. Foxon, and J. J. Harris, Phys. Rev. B **58**, 13 181 (1998).
[12] X. Zianni, P. N. Butcher, and M. J. Kearney, Phys. Rev. B **49**, 7520 (1994).
[13] C. Herring, Phys. Rev. **96**, 1163 (1954).
[14] M. J. Kearney, R. T. Syrme, and M. Pepper, Phys. Rev. Lett. **66**, 1622 (1991).
[15] A. J. Kent, in *Hot Electrons in Semiconductors*, edited by N. Balkan (Clarendon, Oxford, 1988).
[16] B. Tieke, R. Fletcher, U. Zeitler, M. Henini, and J. C. Maan, Phys. Rev. B **58**, 2017 (1999).
[17] P. N. Butcher and M. Tsaousidou, Phys. Rev. Lett. **80**, 1718 (1998).
[18] J. M. Ziman, *Principle of the Theory of Solids* (Cambridge University Press, Cambridge, 1954).
[19] J. H. Davies and I. A. Larkin, Phys. Rev. B **49**, 4800 (1994); S. Chowdhury, C. J. Emeleus, B. Milton, E. Skuras, A. R. Long, J. H. Davies, G. Pennelli, and C. R. Stanley, *ibid.* **62**, R4821 (2000).
[20] A. D. Mirlin and P. Wölfle, Phys. Rev. Lett. **78**, 3717 (1997).
[21] A. D. Mirlin and P. Wölfle, Phys. Rev. B **58**, 12986 (1998).
[22] M. Prasad and M. Singh, Phys. Rev. B **29**, 4803 (1984).
[23] P. M. Morse and N. Feshbach, *Methods of Theoretical Physics* (McGraw Hill, London, 1953), Vol. I, p. 557.
[24] Milton Abramowitz and Irene Stegun, *Handbook of Mathematical Functions* (National Bureau of Standards, Washington, DC, 1972); the identity $\Gamma(1+i/\omega_c\tau)\Gamma(1-i/\omega_c\tau)=(\pi/\omega_c\tau)/[\sinh(\pi/\omega_c\tau)]$ is also being used.
[25] W. H. Press, S. A. Teukolsky, W. T. Vetterling, and B. P. Flannering, *Numerical Recipes in C*, 2nd ed. (Cambridge University Press, Cambridge, 1994), Chap. 9.
[26] The same is true when ∇T changes sign.
[27] M. D'Iorio, R. Stoner, and R. Fletcher, Solid State Commun. **65**, 697 (1988).